

Hai-Yan Xu<sup>1,\*</sup>,  
Jin-Hua Jiang<sup>2</sup>,  
Nan-Liang Chen<sup>2</sup>,  
Fang-Bing Lin<sup>2</sup>,  
Hui-Qi Shao<sup>2</sup>

# Finite Element Modeling for the Uni-Axial Tensile Behaviour of Metallic Warp-Knitted Fabric

DOI: 10.5604/01.3001.0011.5738

<sup>1</sup> Quanzhou Normal University,  
College of Textile and Apparel,  
Quanzhou Fujian, P.R. China;  
\* E-mail: xuhaiyan@qztc.edu.cn

<sup>2</sup> Donghua University,  
College of Textiles,  
Shanghai, P.R. China;

## Abstract

The finite element analysis method (FEM), for its advantages of lower time and economic costing in predicting the mechanical properties of fabrics, was applied to warp-knitted fabrics. In this paper, two bar warp-knitted fabric knitted with wires was used as reflecting mesh antennas. Firstly the loop unit of the metallic warp-knitted fabric was simulated in 3-D by TexGen software. Secondly the 3-D loop unit model was inputted into ABAQUS software to form a model of the metallic warp-knitted fabric sheet for uni-axial tension analysis. Thirdly numerical results were obtained after setting the parameters in ABAQUS. Finally numerical results were verified by uni-axial tensile experiments on the metallic warp-knitted fabric. The results showed that the simulation was in good agreement with the experimental tensile process, where the transfer of yarns between loops when in low fabric elongation and in yarn elongation when in high fabric elongation were simulated by FEM of warp-knitted fabric in the tensile process. Also the same trend of tensile force was found in experiment and FEM results. Therefore it can be concluded that FEM can be used to predict the mechanical properties of warp-knitted fabric with a complex structure.

**Key words:** warp-knitted fabric, finite element analysis, tensile behavior, metallic, TexGen.

## Introduction

Metallic warp-knitted fabrics, a mature application as reflecting surfaces, have been frequently used as deployable mesh reflectors in antennas [1-3]. Such warp-knitted structures have unmatched advantages in the production of mesh structures [4]. Moreover, compared with other mesh structures produced by weaving or weft-knitting, warp-knitted mesh structures as a reflector have more advantages in performance, such as a stable mesh structure and good mechanical properties [5]. Deployable mesh reflector antennas undergo the processes of ground debugging, delivery vehicles carrying and space operation when in use [6]. Thus the mechanical properties are important in metallic warp-knitted fabrics as reflecting surfaces. However, the economic and time costs of experimental analysis for designing reflecting surfaces are too much high due to the complex process of warp knitting and the expensive materials. The finite element method (FEM), a kind of modern numerical simulation method, is considered to be economical in predicting the fabric mechanical properties of fabrics, and has drawn more and more attention in the textile industry.

Compared with woven fabrics, knitted fabrics have a more complex loop struc-

ture, especially warp-knitted fabrics, with each loop interlaced by four other yarn segments, with no quarter loops nor symmetrical half loops. Current research of FEM in warp-knitted fabrics has mainly focused on multi-axial warp-knitted fabrics and warp-knitted spacer fabrics. For structural characteristics, finite element models of multi-axial warp-knitted fabrics and warp-knitted spacer fabrics can be simplified to a unit cell model [7-9]; and even in some models loops can also be simplified [8, 9]. While in basic warp-knitted fabrics, the unit cell is difficult to obtain, and the loop as the fundamental unit cannot be simplified. Several studies concerning mechanical analysis of the basic warp-knitted structure by FEM have been reported. Argyro [10] studied the main deformation mechanism of two bar warp-knitted fabric during tensile tests along the warp and weft direction by FEM, in which numerical methods were considered as an available tool for micromechanical analysis of complex textile, such as warp-knitted fabrics, and can be used in the textile design procedure. Toghchi [11, 12] studied the uni-axial tensile behaviour of single bar warp-knitted fabric in low strain by finite element modelling regarding the loop in the fabric as a twisted sharp of the two-dimensional elastica curve, and concluded that under low strain the model results were more consistent with those of the experiments.

In this study, FEM was adopted to predict

the uni-axial tension behaviour under large elongation of reverse locknit fabric knitted from gild molybdenum wires. The numerical results were verified by comparing with those of experiments, which proved the feasibility of predicting the mechanical properties of basic warp-knitted fabrics using FEM.

## Geometry modelling of metallic warp-knitted fabric

### The loop geometry in metallic warp-knitted fabric

Reverse locknit fabric was knitted from gild molybdenum wires on an RES2 warp-knitted machine. The real shape of the loop in the two-bar metallic warp-knitted fabric is shown in **Figure 1**. It can be seen that loops in the actual fabric are offset with a three-dimensional shape. The distance between courses ( $c$ ) and that between wales ( $w$ ) of the fabric were measured, where  $c$  is 1.16 mm and  $w$  is 1.11 mm.

### Geometry modelling of the loop by using TexGen software

A 3-D geometry model of metallic warp-knitted fabric was established based on the wire properties and actual loop sharp in the fabric [13]. Firstly the 2-D loop geometry was described, shown in **Figure 2**, on basis of the yarn property effect on the loop sharp and underlap as an arc. Where  $b$  is the loop height, and  $n$  the number of wale spaces that the un-

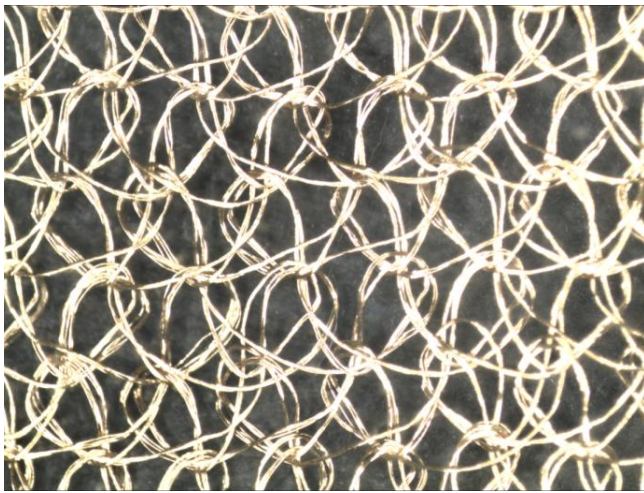


Figure 1. Face view of metallic warp-knitted fabric.

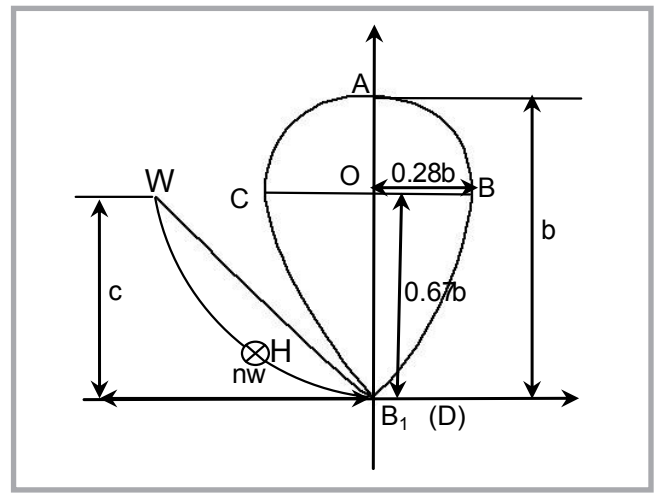


Figure 2. 2-D loop model of metallic warp-knitted fabric.

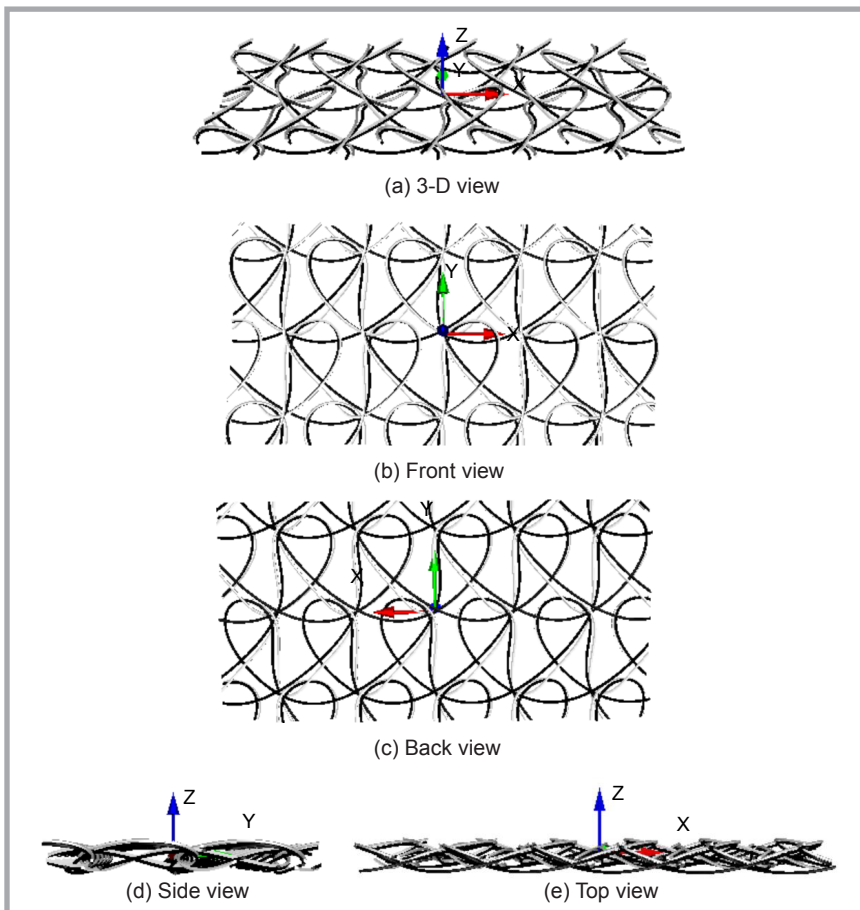


Figure 3. 3-D simulation of metallic warp-knitted fabric.

Table 1. 3-D coordinates of databases in loop.

Databases	Front bar loop	Back bar loop
$B_1$	$(0, 0, 3d)$	$(0, 0, 2d)$
$C$	$(0, 0.73b, 1.5d-0.1b)$	$(0.04b, 0.73b, 0.5d-0.1b)$
$A$	$(0.39b, 0.92b, 1.5d)$	$(0.39b, 0.92b, 0.5d)$
$B$	$(0.52b, 0.51b, 1.5d+0.1b)$	$(0.5b, 0.53b, 0.5d+0.1b)$
$D$	$(0, 0, d)$	$(0, 0, 0)$
$H$	$(-0.5nw, s, -3d)$	$(-0.5nw, s, -4d)$
$W$	$(-nw, c, 3d)$	$(-nw, c, 2d)$

derlap passes. Secondly the angle of loop offset was obtained by stress analysis as  $23^\circ$ . Thirdly the 3-D loop geometry was fixed according to the angle between the loop plane and fabric plane, which was  $20^\circ$ , the yarn diameter, types of loop (front bar or back bar loop), and so on. Finally the coordinates of databases in the 3-D loop model were obtained, shown in **Table 1**, and inputted in TexGen software to simulate the 3-D structure of metallic warp-knitted fabric. Where  $d$  is the diameter of wires, and  $s$  is equal to  $0.5c - 0.21\sqrt{c^2 + n^2w^2}$ . The simulation images in **Figure 3** are similar to the actual fabric, shown in **Figure 1**. In **Figure 3**, the loops in light color were front bar loops, and those in a deep colour were the back bar loops. Also it can be seen that yarns in the simulation images are smooth and independent, thus the 3-D geometry model can be used with FEM. Moreover TexGen software (University of Nottingham, England) was compatible with ABAQUS software (Dassault SIMULIA, France), and the simulation model in TexGen could be inputted to ABAQUS.

### Finite element analysis using ABAQUS software

#### Export of the geometry model from TexGen

Because of the complexity of the warp-knitted structure, the output of the fabric took a long time, and would make some errors in software due to the reverse data. Thus the unit loop in the reverse locknit, shown in **Figure 4**, was exported and rebuilt as a fabric sheet in ABAQUS.

The model in TexGen could be exported

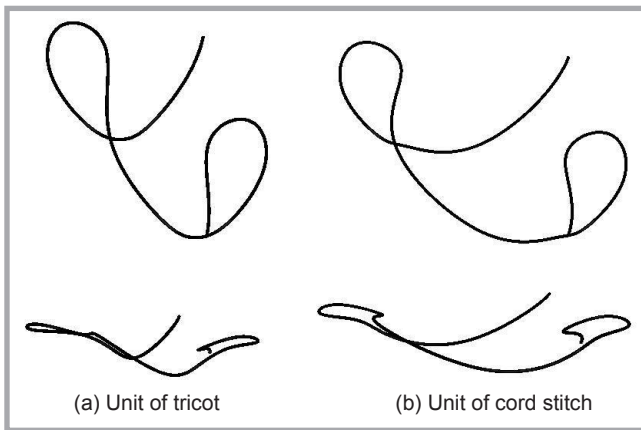


Figure 4. Unit loop in reverse locknit output by TexGen.

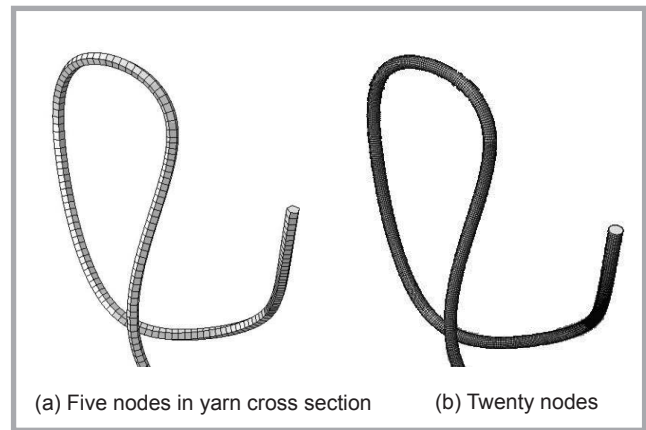


Figure 6. Geometry model formed by facets in ABAQUS.

in several file formats, such as In-House, IGES File, STEP File, Surface Mesh, Volume Mesh, Texgen Mesh and ABAQUS File. The IGES File, STEP File and ABAQUS File could be imported to ABAQUS, while the model exported as ABAQUS File could not be re-meshed in ABAQUS. Compared with the model exported as IGES File and STEP File, the latter was more accurate in describing the model. Thus the STEP File was chosen as the output file in the model.

When exported as the smooth option, shown in Figure 5, in TexGen, there were some errors or distortions of the output model. When the faceted option was chosen to export, the output yarn was made up of quadrilateral facets in ABAQUS, shown as Figure 6. The number of nodes in the yarn cross section was decided by the programming language in TexGen. The number of nodes is 5 in Figure 6.a and 20 in Figure 6.b. Of course, the more nodes in the yarn cross section, the better the description of the model. While the more nodes there were, the bigger the file size was. In this model, 5 nodes were chosen

to describe the loop model.

#### Establishment of a geometry model of warp-knitted fabric in ABAQUS

Firstly the file format was outputted by TexGen to describe the geometry model of the unit cell in the reverse locknit fabric, which was then inputted to ABAQUS to form the model shown in Figure 7.a. Secondly the unit cells were merged in ABAQUS, shown in Figure 7.b. Thirdly a fabric sheet was formed by an array in ABAQUS, shown in Figure 7.c. Finally some parts were cut to form a warp-knitted fabric sheet in ABAQUS for uni-axial tensile analysis, shown in Figure 7.d.

#### Analysis method

ABAQUS/Standard and ABAQUS/Explicit were two major analysis modules. In this model, there were complex interface and nonlinear large deformation in the uni-axial tensile behaviour of the warp-knitted fabric. Thus, to avoid difficulty convergence and improve calculation efficiency, ABAQUS/Explicit was chosen to analyse the model.

#### Material

It was supposed that the gild molybde-



Figure 5. Output options of STEP file in TexGen.

num wire in this study was homogeneous and isotropic. The cross section shape was assumed to be a circle. The mechanical parameters of the material could be got from the tensile behaviour of the wire, shown in Figure 8. Young's modulus  $E$  was calculated directly from the strength-strain curve of the yarn by examining the gradient of the initial curve

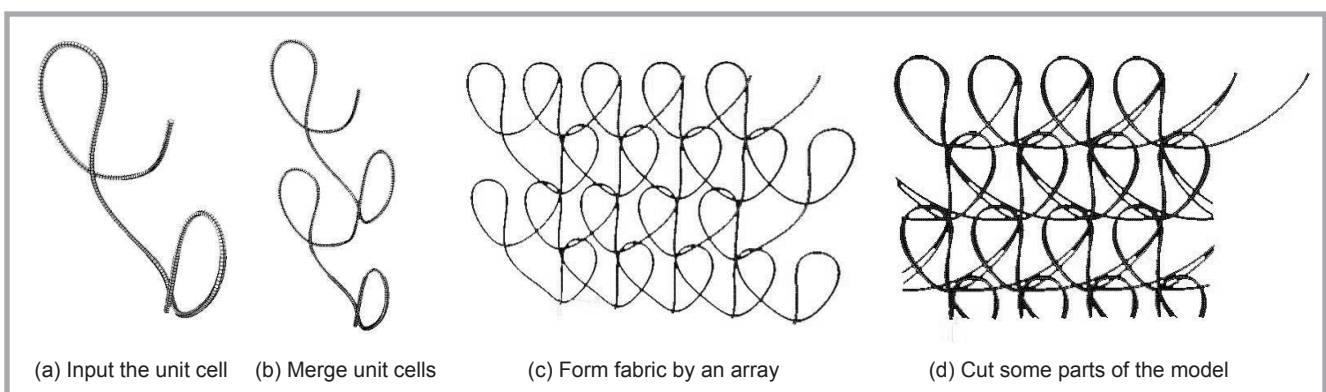


Figure 7. Forming a model of the warp-knitted fabric sheet in ABAQUS.

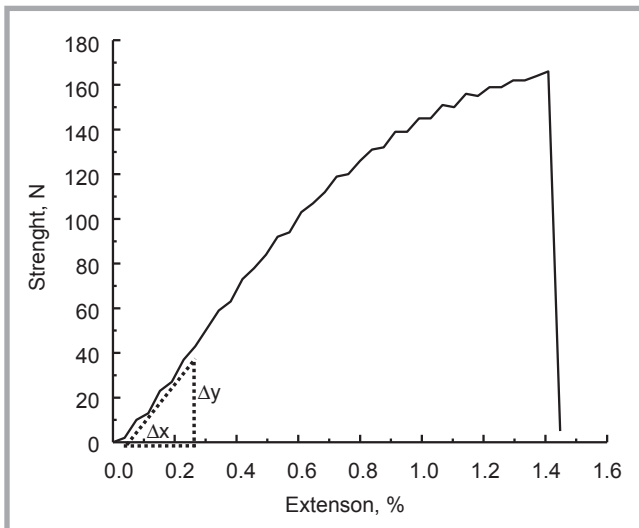


Figure 8. Tensile properties of gild molybdenum yarn.

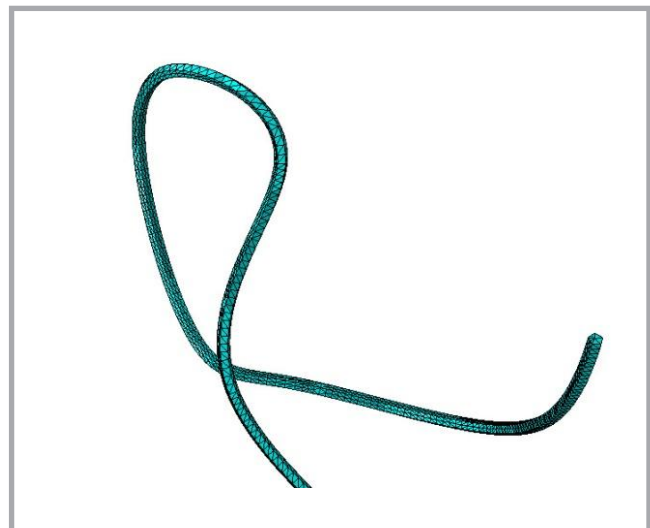


Figure 9. Mesh of fabric in ABAQUS.

segment using *Equation (1)*.

$$E = (\Delta y / \Delta x) / (\frac{\pi d^2}{4}) = 120 \text{ Gp} \quad (1)$$

Poisson's ratio, which was proved to have little effect on the numerical calculation by subsequent analysis, was assumed here to be same for the mental material (0.2~0.3).

### Mesh

The geometry model of yarns in the warp-knitted fabric was complex. Due to the flexibility of free mesh in the element meshing technique, an arbitrary shape can almost be meshed [14]. The C3D10M element in free mesh was suitable for ABAQUS/Explicit [15]. Also it had high accuracy of calculation, but at a large computational cost. In the model, when the C3D10M element was chosen for analytical calculation, the calculation speed was too low to cause analysis error. Thus the standard linear 3D stress ele-

ment C3D4 (a 4-node linear tetrahedron) in free mesh was chosen for mechanical analysis, shown in *Figure 9*.

### Interface friction

The interface friction developed between the yarns was a major contributor to the non-linear uni-axial tensile behaviour of the warp-knitted fabric. The coefficient of friction between yarns (*CF*) was defined as the roughness of the fibre surface. The *CF* between yarns was tested at 0.49 according to ASTM D3412-01.

### Loading

To set the load and restraint conditions of the model as uni-axial tensile process, two ends of the fabric in the transverse direction were fixed separately, one end of the unit cell in the longitude direction except the direction of *y*-axis was fixed, and the other end in the longitude direction was given a displacement. The finite discretization of fabric and the boundary condition were shown in *Figure 10*.

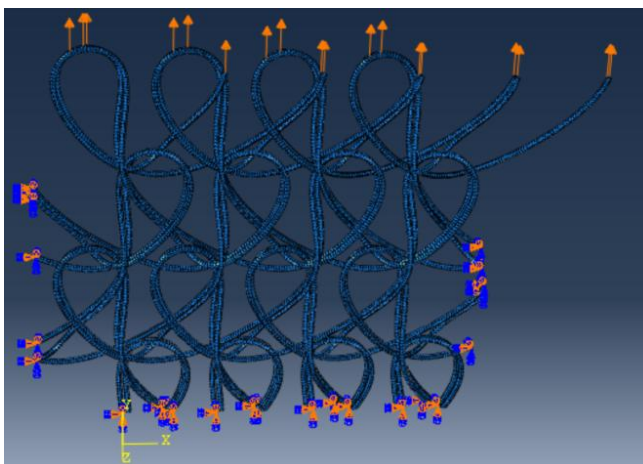


Figure 10. Load and restraint conditions of fabrics.

## Experimental verification

### Experimental results versus numerical results

From *Figure 11*, when the elongation of warp-knitted fabric was less than 20%, the yarns in the underlap were transferred into stitches, and the position of the contact points of stitches between the adjacent courses were changed to the middle of the stitch; thus in this process the friction between yarns was the main contribution to the tensile force of the fabric. When the elongation of warp-knitted fabric was more than 20%, the transfer of yarns in the fabric was finished and the yarns began elongation; therefore the tensile forces of yarns were the main contribution to that of the fabric. Also it could be seen that the experimental tensile process was a good match with the simulated one.

Comparing with the experimental force-strain curve of the warp-knitted fabric for a complex structure and the uncertain stress area, the numerical stress-strain curve of the fabric was also studied. It was found that when the elongation was less than 20%, the force in the experiment and the stress in the simulation increased slowly, shown in *Figure 12* and *Figure 13*, and these were in good agreement with the tensile process analysis. Moreover from *Figure 12* and *Figure 13* it is seen that the trend of the experimental force and that of the numerical stress were consistent. When the elongation was more than 20%, the increasing amplitude of the numerical stress was more than that of the experimental force as the stress area was smaller along with yarn stretching.

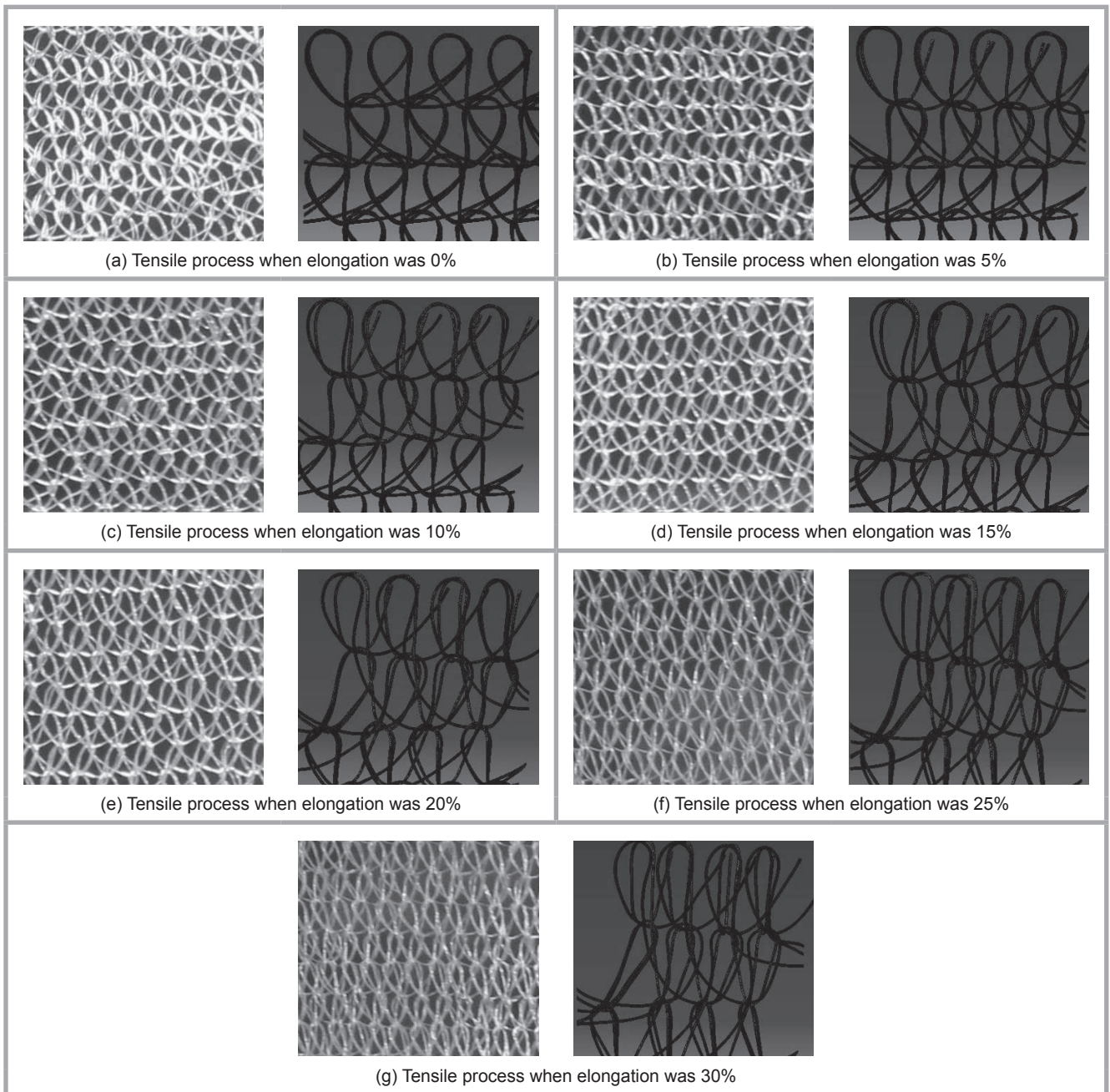


**Figure 11.** Experimental versus numerical tensile process.

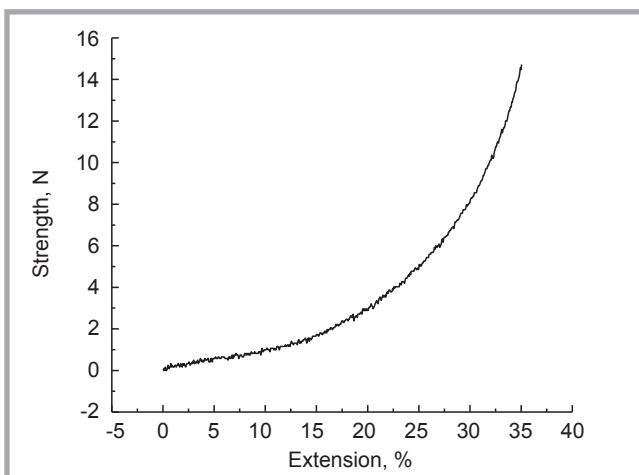


**Figure 12.** Experimental force-strain curve of fabric.

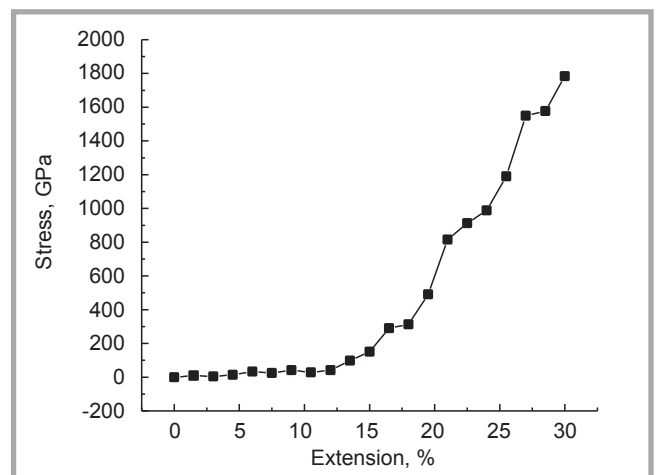


**Figure 13.** Numerical stress-strain curve.

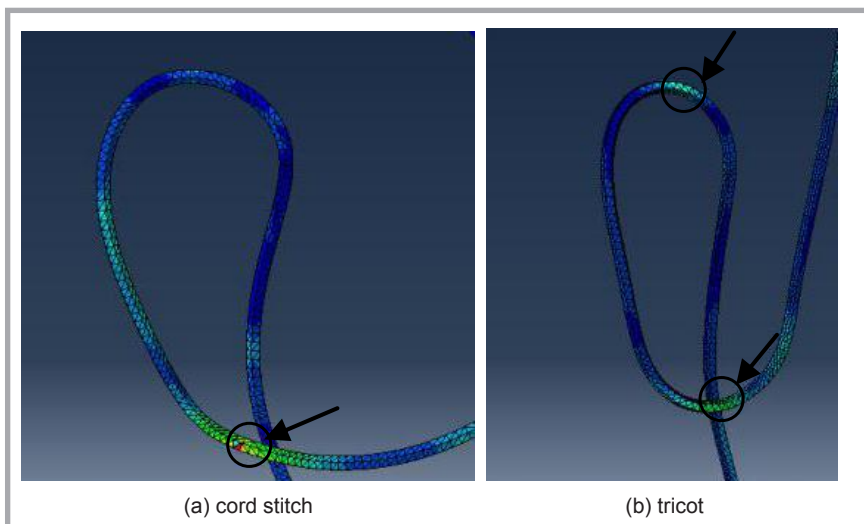


Figure 14. Stress distribution in fabric.

### Stress distribution

The single loop was shown to find the stress distribution, given in **Figure 14**, and the red and yellow areas displayed in the circle were the stress concentration areas. It was observed that the maximum stress was mainly located in the area of yarn contact, where significant loop curvature and yarn slippage happened during loading.

By examining the highly stressed areas, the failure regions were well predicted by FEM. The analysis showed that the areas of yarn contact were the most critical regions, with high stress concentration, generated by the compound forces of bending, compressing and abrading.

### Conclusions

In this study, a geometry model of warp-knitted fabric was simulated by TexGen software, and then the model was outputted to ABAQUS. The uni-axial tension of the warp-knitted fabric was analysed by FEM. The results showed that FEM was feasible for warp-knitted fabric with a complex structure to predict its mechanical properties.

- Some databases on the geometry model describing the unit cell of warp-knitted fabric were obtained and inputted to TexGen software to simulate the 3-D geometry of the loop. And the geometry model was outputted from TexGen and then inputted to ABAQUS. Then a finite element model of uni-axial tension of the warp-knitted fabric was established by definition of the material, mesh, loading, interface friction, and so on, in ABAQUS.
- The results of experiments and finite element analysis of uni-axial tension were studied. In the numerical analysis of warp-knitted fabric in the tensile process using FEM, the transfer of yarns between loops and yarn elongation when at different fabric elongations were simulated. The simulation was in good agreement with the experimental tensile process. Also the same trend of the tensile force was found in experiment and finite element analysis. It was also observed that the maximum stress was mainly located in the area of yarn contact, where significant loop curvature and yarn slippage happened during loading.

### Acknowledgements

This work was financially supported by the National Key R&D Program of China (2016YFB0303300), the Natural Science Foundation of China (NSFC 11472077), and by the Fundamental Research Funds for the Central Universities (2232015D3) and CNTAC J201507.

### References

1. Miura A, Tanaka M. Antennas and Propagation Society International Symposium, 2004, (1), 33-36.
2. Boan B J, Schwam M, Sullivan M R, et al. *Gold-plated tungsten knit RF reflective surface: US*, US4609923[P]. 1986.
3. Miura A, Rahmat-samii Y. *IEEE Transactions on Antennas and Propagation* 2007, 55(4): 1022-1029.
4. Bassily S F, Uribe J. *Method of marking tensioned mesh for large deployable reflectors: US*, US6214144B1[P], 2001.
5. Jia W. Development and Research for the Mesh Materials of the Large Deployable Reflector Antenna [D]. Shanghai: Donghua University, 2011.
6. Zhen J, Li D, Tian Y, et al. *Electro-Mechanical Engineering* 2005; 2(3): 49-55.
7. Zhang F, Wan Y. *Knitting Industries* 2014; (4): 23-26.
8. Vassiliadis S, Kallivretaki A, Psilla N, et al. *FIBRES & TEXTILES in Eastern Europe* 2009;76(5): 56-61.
9. Zhang T, Yan Y, Liu B, et al. *Acta Materialiae Sinica* 2013; 30(5): 236-243.
10. Argyro K, Savvas V, Mirela B, et al. *RJTA*, 2007, 11(4): 40-47.
11. Toghchi M J, Ajeli S, Silami M, *Journal of the Textile Institute* 2012; 103(5), 477-482.
12. Toghchi M J, Ajeli S. *Journal of textiles and polymers* 2013; 1(1): 31-35.
13. Xu H, Chen N, Jiang J, et al. *Journal of the Textile Institute* 2017; 108(3): 368-375.
14. Sun L, Chen Z, Ma J. *Shandong Textile science & technology* 2008; 49(5): 51-54.
15. Zhuang Z, Zhang F, Cen S. *Nonlinear finite element analysis and examples in ABAQUS*, Beijing, Science Publishing Company, 2005.



Received 14.03.2016 Reviewed 25.10.2017

# MoDeSt2018

The 10th International Conference of Modification, Degradation and Stabilization of Polymers

2-6 September, 2018  
The University of Tokyo, Tokyo, Japan